



An Efficient Classification and Segmentation of Brain Tumor Images Using Fuzzy Approach with Optimization Technique

M. P. Thiruvenkatasuresh^{1,*} and V. Venkatachalam²

¹Department of Computer Science and Engineering, Excel Engineering College, Komarapalayam, Namakkal 637303, Tamilnadu, India
²Erode Sengunthar Engineering College, Thudupathi Post, Perundurai, Erode 638057, Tamilnadu, India

In numerous uses of image processing and computer vision, it is image segmentation that is generally utilized. A given image is divided to distinctive areas by utilizing the division procedure taking into account some decisive factors. The investigation of the Computed Tomography (CT) images considers image division a critical and imperative part in recognizing the various types of tumor. The tumor's grouping and the non-tumor images took after by the segmentation of tumor locale in CT images is finished by the proposed methodology. The process of classifying is carried out by Adaptive Neuro-Fuzzy Inference System (ANFIS) classifier. It combines the explicit knowledge representation of an FIS and the learning power of the artificial neural networks. After the classification segmented the tumor part of the image, here fuzzy, c means clustering (FCM) technique with centroid optimization. As regards the centroid optimization Gray Wolf Optimizer (GWO) are used to increase the accuracy of the proposed approach. An accuracy rate of 99.24% in the analysis of the segmentation process is obtained Using GWO technique and Proposed FCM approach compared to existing technique the accuracy is 57.7%. It is in the working platform of MATLAB that this proposed methodology is implemented.

Keywords: Brain Image, Feature Extraction, Tumor, Classifier, Adaptive Neuro Fuzzy Inference System, Segmentation, Grey-Level Run-Length Matrix (GLRLM).

1. INTRODUCTION

Image processing is regarded to be a standout amongst the most rapidly creating horizons of information technology, with mounting applications in all areas of learning. It speaks to a center point of examination inside of the computer science given the noteworthiness of potential applications extending from image enhancing robotics and computer vision.¹ Extended image segmentation serves a vital purpose in the entire image scrutiny along with the computer perspective. Partitioning an image in image segmentation in terms of typical homogeneous qualities such as intensity, color, tone etc. is presented.² In furtherance, segmentation is the starting point for the other functions such as image registration, shape analysis, visualization, and quantitative analysis. The configuration of the brain may easily be analyzed by the Magnetic Resonance Imaging (MRI) scan or Computed Tomography (CT) scan. The former has an edge over the latter in terms of easiness for assessment. Further it does not adversely affect the human body as it is devoid of radiation and is wholly dependent on the magnetic field and radio waves.³

In the biomedical applications, mechanical retinal image assessment distinguished the retinal pathologies effortlessly for the ophthalmologists, though the conventional methods like the dilation of the eye pupil, involved significant period of time with the chaperon bothers for the patients concerned.⁴ The Medical imaging has effected an ocean change in the social insurance science. The developments in medical imaging have produced quicker and further exact imaging which is less tenuous. This has brought about the broad livelihood of the imaging for different circumstances and various patients.⁵ The general post-processing routines in the thermal imaging, utilized in the image evaluation, comprise of high-pass filters proposed for recognizing the hot or cold spots, temperature averaging and figuring spatial, temporal or frequency changes of temperature.⁶ The Near-infrared (NIR) tumor imaging has developed as an engaging non-invasive method. The arrangement of the NIR cyanine dyes as differentiating specialists is followed by assorted groups, which incorporate our group moreover. Different particular attributes of these dyes adjust them essentially suitable for the tumor imaging.⁷

The fractal and multi-fractal assessments of the human retinal vascular network by and large depend on the investigational

*Author to whom correspondence should be addressed.

and useful limitations like the variety of subjects, image acquirement, kind of image, image processing, fractal and multi-fractal approaches, together with the technique and specific computation deployed.⁸ If a distinguished pathogen does not come under the umbrella of at least one of these three ailments, the relative image is classified as being tainted by a strange ailment. It is built up that the decay of the image to be sorted in color elements, is liable to result in the productive order of the natural objects.⁹ Both animal and human brain imaging examinations have delineated the contribution of the amygdala with regard to fear training. Consistent with its commitment in the domain of fear acquirement, particular sores of the amygdala caused damage to the fear processing task.¹⁰ Many an endeavor has been made to find the neurobiological corresponds of neuroticism by means of the neuro imaging systems like the positron emission tomography (PET) and functional magnetic resonance imaging (fMRI).¹¹

In such manner, the breast thermography holds immense potential for recognizing the occurrence of well ahead. The temperature allotment of the breast surface assembled by numerical replication as the temperature assessed experimentally, showing that the infrared images could be utilized to complete these evaluations.¹² The key imperatives confronted in the preliminary investigation incorporated the immense dimension of the sensors; inferior resolution, and the limited force of the computers for the image post processing.¹³ As the CMR is encountering uncommon development, the excused suggestions for image attainment, clarification and post processing are required routinely and will be offered by online reference sections when required and upgraded Task Force papers in great time.¹⁴ It must be borne personality a top priority that the preparatory stage ID goes far in sparing the valuable existence of the individuals. The Parkinson's disease specialists are equipped to take proper and auspicious choices by evaluating the test results of the patients concerned. The enhancement of diagnosis and assessment in the preparatory phase of the infirmity is accomplished by the functional Neuro imaging.¹⁵ It was an open-source image processing toolbox mainly committed to the fetal brain MRI. It encompasses an image denoising technique, different image modifying methodology and a probabilistic tractography method.¹⁶

In the mass spectrometry imaging (MS Imaging) a sample of interest is observed and the ensuing particle signals are modernized into a pixel image. With respect to a few analytical techniques, data dispensation has risen as a basic section of the work process for MS imaging.¹⁷ A renovated diffusion technique, suitable for images with inferior-contrast and irregular illumination, was proposed. In the investigation, more noteworthy consideration was given on the discrete execution of the method and the test results of the novel conductance capacities which were suggested.¹⁸ The ultimate aim of outfitting a controlled-access database, open to qualified specialists and clinicians, which has the capacity serve as a dominant gadget for comprehending the characteristic brain development and finding the changes connected with the brain based syndromes and ailments, and as an asset for renovating the computational techniques and image processing devices.¹⁹ Further, certain statistical qualities of the specified zone are framed after locating the tumor region, with an eye on interpreting, scrutinizing, classifying, and recognizing the brain tissues data. It extends a much-needed helping hand to the radiologists, physicians, and surgeons in their judgment tasks,

offering them in a platter palatable data within a reasonable duration of time.

2. LITERATURE REVIEW

In the year 2014, Tayade et al.²⁰ attracted worldwide consideration when he recommended that it was a direct result of the human vision deficiency that we were not able to find in volumes and even we were not ready to distinguish the adjustments in volumes of any image or multiple images. The Image processing was a type of signal processing for which the input was a image, similar to the photograph or video frame. Also, the yield of image processing could be either an image or an arrangement of attributes or requirements connected to the image. Two dimension images like X ray images containing the lung disorders tuberculosis, lung emphysema, pneumonia could be effectively gathered and processed. The work of 3D images from CT scan and MRI is set to toss a few grave difficulties in the treatment treating and diagnosis of ailment identified with the Head and abdomen area. The commitment of image processing is additionally feasible in the disease forecast and as a prognostic device.

In 2014, Bhuvaneswari et al.²¹ splendidly propounded the way that lung infections speaks to the afflictions influencing the lungs, which are the organs enabling the people to breathe and it has risen as the most boundless medical malaise throughout the world, especially in India. The key target of their document was to recognize and classify the lung illnesses by method for efficient feature extraction supported by the minute invariants, feature selection with the help of the genetic algorithm and the results were arranged by the Naïve bayes and decision tree classifiers. It could be enhanced by employing so as to take certain extra lung sicknesses and by employing added feature extraction techniques by incorporating with parallel characterization approaches with an eye on introducing further prevalent and exact results. The decision tree classifier outlined further attractive results opposite those of the naive bayes classifier.

The year 2014 saw Mishra et al.²² suggesting that the medical image processing had outlined multitalented computational and mathematical techniques for determining the difficulties connected to the medical images and their organization for biomedical examination and clinical consideration. The MIP focused on the computational evaluation of the images, disregarding their attainment. The MIP examination was regularly capable to yield a response to the inquiry in regards to the plausible point of interest of a determined MIP issue or an as of late planned MIP-based system supporting an indicative or therapeutic procedure, as to the result benchmarks, for example, the Quality Adjusted Life Years (QALYs) for the patient or expense reserve funds in social insurance.

In 2014, Chavan et al.²³ won name and fame by launching diverse methods to diagnosis malaria of which manual microscopy was esteemed to be the highest quality level. The image based technique was tested in light of more than 30 images from two independent laboratories. Their expectation was to dispatch an incredible, unverified and susceptible malaria screening strategy with unimportant material expense which picked up an unassailable edge over the associate methodologies and had the capacity chopped down the human reliance and was further unswerving in applying diagnosis criteria. The general affect ability to catch instances of malaria was observed to be 100% and

the specificity in the scope of 50–88% for the whole types of malaria parasites.

In 2016 Hung et al.²⁴ have proposed an efficient parallel fuzzy c-means clustering algorithm for segmenting images on multiple embedded graphic processing unit systems, NVIDIA TK1. The experimental results reveal that the extreme speedups of the proposed algorithm on 15 TK1s greater than 12 times and 7 times than that of fuzzy c-means algorithm with single ARM and Intel Xeon CPUs, respectively. These experimental results show that the proposed algorithm can significantly address the complexity and challenges of the brain magnetic resonance imaging segmentation problem.

In 2015 IvanaDespotović et al.²⁵ in the last few decades, various segmentation techniques of different accuracy and degree of complexity have been developed and reported in the literature. In this paper we review the most widespread methods commonly used for brain MRI segmentation. We highlight differences between them and discuss their capabilities, advantages, and limitations. To address the complication and challenges of the brain MRI segmentation problem, we first make known to the basic concepts of image segmentation. Then, we explain different MRI preprocessing steps including image record-keeping, bias field correction, and removal of non-brain tissue. Finally, after go through different brain MRI subdivision methods; we discuss the validation problem in brain MRI segmentation.

3. PROPOSED METHODOLOGY

This methodology comprises an effective technique that can be utilized to classify images as tumor or nontumor and segment the tumor portion from the Computed Tomography (CT) scan Brain images. This process consists of pre-processing, feature extraction, classification and segmentation processes. Initially, the pre-processing steps will be applied over the brain images for enhancing the clarity of the input image; here adaptive median filter is used. The extraction of meaningful information (features) such as Grey-Level Run-Length Matrix (GLRLM) and Maximum intensity (MI) from medical images is carried out. Once the feature extraction is completed the extracted features are used to train the ANFIS classifier. The ANFIS is a Fuzzy Inference System (FIS) implemented in the framework of an adaptive fuzzy neural network. The classification is done in two important phases, namely, the training phase and the testing phase. In the training phase, the classifier is trained with the extracted features of the training data.

After the classification process, for the segmentation of the brain tumor part Fuzzy C-Means (FCM) clustering process along with the optimization method is employed. In the fuzzy clustering, every point has a degree of belonging to the clusters, as in the fuzzy logic, rather than belonging completely too just one cluster. Thus, points on the edge of a cluster may be in the cluster to a lesser degree than the points in the center of cluster. For optimizing the centroid of the FCM Grey Wolf Optimization (GWO) technique is used this algorithm compared to the Particle Swarm Optimization (PSO) algorithm and Ant colony Optimization (ACO). Finally, the optimal centroid is utilized to obtain the extracted tumor part of the image. The proposed scheme attains the maximum accuracy as compared to the Normal FCM process, its implemented using MATLAB. The block diagram of the proposed method is given hereunder in Figure 1.

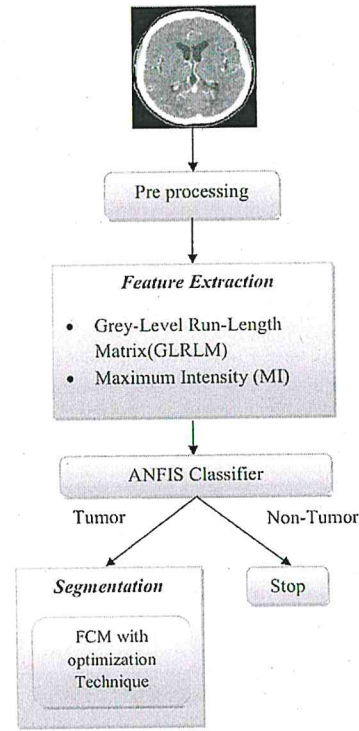


Fig. 1. Block diagram of proposed methodology.

3.1. Preprocessing

Adaptive median filter is used to empower the flexibility of the filter to change its size as needs be founded on the guess of local noise density. The adaptive median filter depends on a trans-conductance comparator, in which immersion current can be altered to go about as a local weight operator. Since the size of the filter is adjusted to the local noise content, this kind of median filter is known as adaptive median filter. This filter, if image is noisy and target pixels neighboring pixel worth is somewhere around 0's and 255's then we supplant pixel esteem with the median value.

Let $S_{i,j}$ which locates at (i, j) , be the gray intensity of a $R \times C$ image S and $\min \max L \times L$ be the dynamic range of S i.e., $\min i, j \max L \leq x \leq L$ for all (i, j) which accords to the following rule:

$$(i, j) \in A = \{1 \dots R\} \times \{1 \dots C\} \quad (1)$$

In the conventional noise model, we assume y is the noisy image, the model is given by

$$y_{i,j} = \begin{cases} L_{\min} & \text{with percentage } p \\ L_{\max} & \text{with percentage } q \\ s_{i,j} & \text{with percentage } 1 - p - q \end{cases} \quad (2)$$

Where rate $p + q$ means the noise level in image and assume the filtering window $W_{i,j}$ is a window of size $(2C + 1) \times (2C + 1)$ centered at position at (i, j) , $W_{i,j}$ can be written as:

$$W_{i,j} = \{s_{i-C, i-C} \dots x_{i,j}, \dots, x_{i+C, j+C}\} \quad (3)$$

Let $w = 2C + 1 \leq W$ max. The filter tries to improve the output image $y_{i,j}$ the median in the window.

3.2. Feature Extraction

The feature extraction technique includes the investigation of the brain CT images and for this image feature extraction the spectral analysis method is conveyed. By feature extraction what is implied is the adaptation of the input data into the set of features. In our examination, the features thought seriously about are

- Grey-Level Run-Length Matrix (GLRLM)
- Maximum intensity (MI).

3.2.1. Grey-Level Run-Length Matrix (GLRLM)

GLRLM is a matrix from which the texture features can be extracted for texture examination. A texture is comprehended as an example of gray intensity pixel in a specific heading from the reference pixels. Run length is the quantity of the nearby pixels that have the same gray force in a specific direction. Gray level run length matrix is a two dimensional matrix where every element $z(i, j/\theta)$ is the number of elements j with the intensity i in the direction θ . The Gray Level Run Length matrix is developed as takes after:

$$K(\theta) = (g(i, j)/\theta), \quad 0 \leq i \leq N_g, \quad 0 \leq j \leq K \max \quad (4)$$

Where N_g the maximum is gray level, $K \max$ is the maximum length and i, j is a matrix size values.

GLRLM obtain more than a few statistics from them employing the grey co-props function. These statistics offer information about the texture of an image. The statistics are such as

- Short Run Emphasis (SRE)
- Long Run Emphasis (LRE)
- Gray-Level Non uniformity (GLN)
- Run Length Non uniformity (RLN)
- Run Percentage (RP)

(a) Short Run Emphasis (SRE)

Short Runs Emphasis (SRE) isolates each run length by the run's length squared. This has a tendency to highlight short runs. The denominator is the total number of runs in the image and serves as a normalizing factor.

$$SRE = \frac{1}{n_r} \sum_{i=1}^G \sum_{j=1}^V \frac{z(i, j)}{j^2} \quad (5)$$

The SRE is highly dependent on the occurrence of short runs and is expected large for fine textures.

(b) Long Run Emphasis (LRE)

Long Runs Emphasis (LRE) increases every run length by the run's length squared. This should emphasis long runs. Measures conveyance of long runs and highly dependent on the event of long runs and is normal extensive for coarse structural textures.

$$LRE = \frac{1}{n_r} \sum_{i=1}^G \sum_{j=1}^V z(i, j) * j^2 \quad (6)$$

(c) Gray-Level Non uniformity (GLN)

GLN Measures the similarity of gray level values throughout the image. The GLN is expected small if the gray level values are alike throughout the image.

$$GLN = \frac{1}{n_r} \sum_{i=1}^G \left(\sum_{j=1}^V z(i, j) \right)^2 \quad (7)$$

(d) Run Length Non uniformity (RLN)

Measures the length's similitude of keeps running all through the image, the RLN is expected little if the run lengths are indistinguishable all through the image.

$$RLN = \frac{1}{n_r} \sum_{i=1}^V \sum_{j=1}^G (z(i, j))^2 \quad (8)$$

(e) Run Percentage (RP)

This feature is the ratio between the total number of watched keeps running in the image and the total number of possible runs if all runs had a length of one.

$$RP = \frac{n_r}{z(i, j) \times j} \quad (9)$$

The homogeneity and the circulation of keeps running of a image in a specific direction the RP is the biggest when the length of runs is 1 for every gray levels in specific direction.

3.2.2. Maximum Intensity (MI)

The most elevated force of the images alludes to the most noteworthy check of pixel qualities (0 to 255) and the accompanying intensity value. The histogram of an image for the most part identifies with a pixel's histogram force values in a image processing connection. What's more, it speaks to a graph portraying the number of pixels in a image at every last special force worth found in the relative image. Because of the fact that there are 256 different achievable intensities for a 8-bit grayscale image, the histogram graphically offers 256 numbers portraying the designation of pixels among those grayscale values.

$$I = \max_{i=0}^{255} (\text{count of pixel intensity}) \quad (10)$$

3.3. Classification Using ANFIS

Adaptive Neuro Fuzzy Inference System is the mix of best features of fuzzy inference system (FIS) and artificial neural network (ANN). It joins the express information representation of a FIS and the learning power of the artificial neural network. The goal of the ANFIS is to coordinate the best features of the fuzzy system and the neural networks. ANFIS serve as a premise for building an arrangement of fuzzy if-then guidelines with suitable enrollment capacities to produce the stipulated input-output pairs. This is a fuzzy inference system with a back engendering that tries to reduce the error and enhances the execution. The block diagram of ANFIS building design is given in Figure 2.

Figure 2 x and y are the crisp inputs. A_i and B_i are the linguistic labels (low, medium, high, etc.) ($i = 1$ or 2) and w is a weight of the ANN process. The organization of ANFIS is comprised of five layered feed-forward neural network is shown in Figure 2. ANFIS architecture consists of five layers of nodes. Out of five layers, the first and the fourth layers acquire adaptive nodes while the second, third and fifth layers acquire fixed nodes.

Figure 3 shows the FIS generation the brain images are considered to classify the tumor and non tumor images and the rules based on Sugeno's fuzzy model and specified the image classification. In both neural network (NN) and fuzzy logic (FL), the inputs are given to the input layer (as input membership function) and the output is attained from the output layer (as output

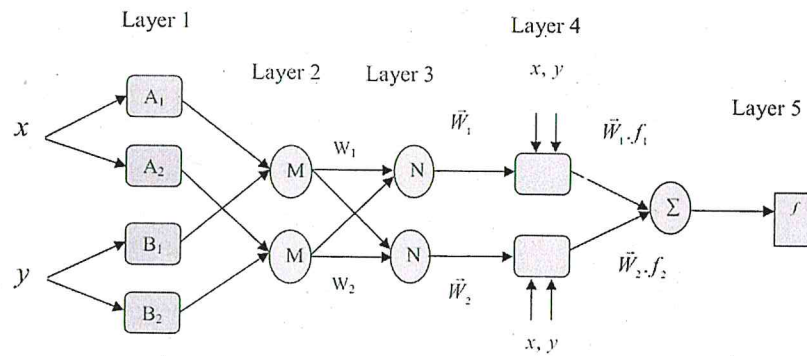


Fig. 2. ANFIS architecture.

membership functions). In the ANFIS, nodes in the same layer have similar functions as described below:

Layer 1 (Input nodes): Nodes of this layer create membership grades of the crisp inputs which have a place with each of convenient fuzzy sets by utilizing the membership functions. The produced bell-shaped membership function given below equation

$$\delta_A(x) = \frac{1}{1 + ((x - c_i)a_i)^{2b_i}} \quad (11)$$

Where δ_A the appropriate membership is functions for A_i fuzzy set, a_i , b_i and c_i is the membership functions parameter set (premise parameters) that changes the shape of membership function from 1 to 0.

Layer 2 (Rule nodes): In this layer, the rule operator (AND/OR) is applied to get one output that represents the results of the antecedent for a fuzzy rule. The outputs of the second layer, called as firing strengths O_i^2 are the products of the incoming signals obtaining from layer 1, named as w in below

$$O_i^2 = w_i = \delta_A(x)\mu_B(x); \quad i = 1, 2 \quad (12)$$

Image classification process in ANFIS rules is generated. Each rule contains the unity weight and the learning process of ANFIS is carried out on the classified images.

Layer 3 (Average nodes): In this layer, the nodes calculate the ratio of the i th rules firing strength to the sum of all rules firing strengths.

$$O_i^3 = w_i = \frac{w_i}{\sum_i w_i} \quad (13)$$

Layer 4 (Consequent nodes): In this layer, the contribution of i th rules towards the total output or the model output and/or the function calculated as follows:

$$O_i^3 = \bar{w}_i f_i = w_i(p_i x + q_i y + r) \quad (14)$$

Where, w_i is the output of Layer 3 and p_i , q_i , r_i are the coefficients of linear combination in Sugeno inference system. These parameters of this layer are referred to as consequent parameters.

Layer 5 (Output nodes): This layer is called as the output nodes. This layer's single fixed node computes the final output as the summation of all incoming signals.

$$O_i^5 = f(x, y) = \sum \bar{w}_i f_i \quad (15)$$

$$f_i = p_i x + q_i y + r \quad (16)$$

In the fifth layer, there is a fixed node. This node creates the output by summing every single approaching signals. The learning calculation for ANFIS is a hybrid algorithm, which is a blend between inclination drop and slightest squares strategy for distinguishing nonlinear input parameters a_i , b_i and c_i and the linear output parameters separately. The ANFIS demonstrating performed utilizing the “subtractive fuzzy clustering” function as which can perform effectively even in less standards.

The last stage output of ANFIS minimizes the error signal, which is accurately named non tumor and tumor images. The execution of ANFIS is tested by giving more number of signals.

3.4. Segmentation Process

In this area, we have viably isolated the tumor image with the assistance of the mighty fuzzy C means grouping (FCM) technique with the optimization procedure. It is a delicate (fuzzy) division strategy that holds considerably more data than hard division strategies. It provides flexibility through fuzzy classification of pixels where pixels are permitted to have a place with various clusters with an membership degree somewhere around

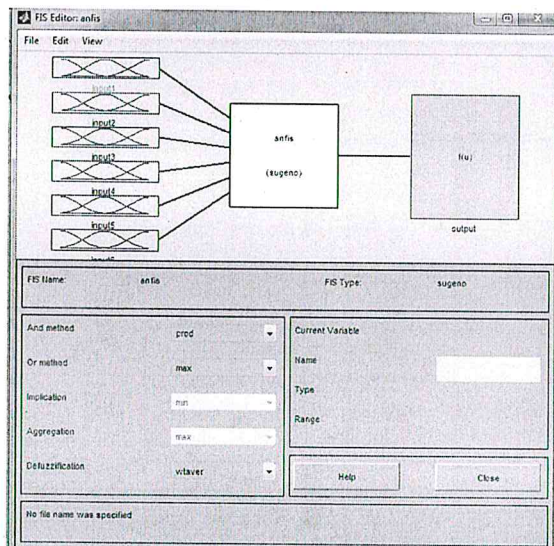


Fig. 3. Structure of FIS generation.

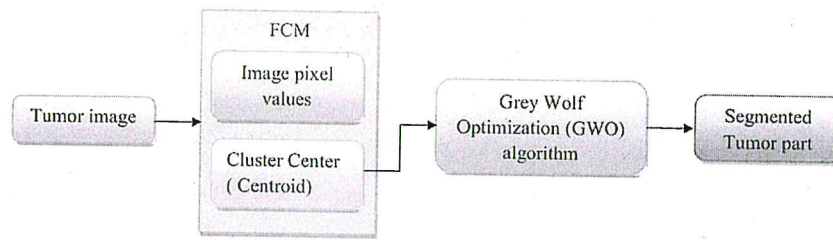


Fig. 4. Segmentation process.

0 and 1. The algorithm is an iterative advancement that minimizes the objective function. The FCM is generally utilized for clustering where the execution of the FCM relies on upon the determination of initial cluster center or membership value to the tumor image pixel values. The FCM algorithm begins with an arrangement of initial cluster centers (or) arbitrary membership values. For optimize the cluster center utilizing Grey Wolf Optimization (GWO) technique. The tumor's characterization image is assigned as the input to the division process to coerce the tumor piece of the image, which is exhibited in Figure 4.

3.4.1. Fuzzy C Means Clustering (FCM) Process

Fuzzy c-means algorithm permits data to have a place with two or more clusters with different membership coefficient. Fuzzy C-Means clustering is an iterative procedure. To start with, the beginning fuzzy partition matrix is created and initial fuzzy cluster centers are computed. In every progression of the iteration, the cluster centers and the membership grade point are overhauled and the objective function is minimized to locate the best area for the clusters. FCM algorithm steps are given underneath. FCM has been utilized with some accomplishment as a part of the delicate division of MR images and for the estimation of partial volumes. It is formulated as the accompanying minimization objective function concerning the membership function u and the centroids v .

The parameter m controls the fuzziness of the subsequent segment, and $m = 2$ is utilized as a part of this study. The objective function is minimized when pixels near the focuses of their clusters are relegated high membership values, and low membership values are allotted to pixels with far from the focuses of their clusters. The membership function speaks to the probability that a pixel fits in with a specific cluster.

Steps

1. Let $x = \{x_1, x_2, \dots, x_n\}$ be the set of data points and $c = \{c_1, c_2, \dots, c_n\}$ be the set of centers.
2. For select the cluster centre or centroid in the segmentation process using GWO technique.
3. Compute the objective function of the Fuzzy process using below function

$$J_m = \sum_{i=1}^n \sum_{j=1}^c u_{ij}^m \|x_i - c_j\|^2 \quad (17)$$

4. calculate the fuzzy membership function u_{ij} using

$$u_{ij} = \frac{1}{\sum (d_{ij}/d_{ik})^{2(m-1)}} \quad (18)$$

5. Compute the fuzzy centers c_j

$$c_j = \left(\frac{\sum_{i=1}^n (u_{ij})^m x_i}{\sum_{i=1}^n (u_{ij})^m} \right) \quad \forall j = 1, 2, \dots, c \quad (19)$$

6. Repeat step 4 and 5 until the maximum of J_m value is achieved or $\|U^{(k+1)} - U^k\| < \beta$.

Parameter Explanation of above equation

J	Objective function
m	Fuzziness index $m \in [1, \infty]$
n	Data points
u_{ij}	Membership of i th data to j th cluster center.
c	Number of cluster center.
d_{ij}	Euclidean distance between i th data and j th cluster center.
c_j	j th cluster center
k	Iteration step
β	Termination criterion between $[0, 1]$.
U	$(u_{ij})_{n \times c}$ is the fuzzy membership matrix.

3.4.2. Centroid Optimization Using GWO

This process is carried out to attain the segmented image, and for the purpose, the optimization technique is applied. In the centroid optimization the maximum accuracy is obtained in the GWO.

Pseudo code for GWO

Step 1: Initialize the solution $c_i = (1, \dots, n)$. Initialize a , A , and C

Step 2: Find the fitness of the initial solution

$$F_i = \max \left(\frac{TP + TN}{TP + TN + FP + FN} \right)$$

Step 3: Separate the solution based on the fitness

- c_α = the first best search solution
- c_β = the second best search solution
- c_δ = the third best search solution

Step 4: Update the position of the current search solution

$$c(t+1) = \frac{\vec{c}_1 + \vec{c}_2 + \vec{c}_3}{3}$$

Step 5: Calculate the fitness of the new search solution

$$F_i(\text{new}) = \max \left(\frac{TP + TN}{TP + TN + FP + FN} \right)$$

Step 6: Store the best solution so far attained

Iteration = Iteration + 1

Step 7: Stop after the optimal solution is attained.

The grey wolves adequately frame a Canidae's piece family and are esteemed as the apex predators showing their position at the sustenance's food chain. They routinely show an inclination to make due as a group. The heads constitute a male and a female, labeled as alpha, which are for the most part in charge of taking suitable choices viewing different factors, for example, the hunting, sleeping place, time to wake, and so forth. The choices made by the alpha are passed on to the group.

The Beta speaks to the second rank in the pecking order of the grey wolves. They are, basically, auxiliary wolves which adequately offer some assistance to the alpha in the choice making or comparable group functions.

The omega, which is at the least strata of the grey wolf pack, by and large functions as a substitute offering into the other leading wolves very nearly on each event and are permitted to have just the little scraps taking after a great blowout by the leader wolves. A wolf is marked as subordinate or as delta every so often in the event that it doesn't fit in with the gathering of an alpha, beta, or omega. In spite of the fact that these delta wolves need to respect the alphas and betas, they, then again, have a successful predominance over the omegas. In our technique, the alpha (α) is esteemed as the most suitable arrangement with a perspective to replicating logically the social pecking order of wolves while conceiving the GWO. Thus, the second and the third best arrangements are named as beta (β) and delta (δ) separately. The remaining applicant arrangements are regarded to be the omega (ω). In the GWO method the hunting (optimization) is guided by the α , β , δ and ω .

3.4.2.1. Initialization Process. In the district developing procedure, we pick the seed point and the centroid fragment the image. Here we introduce the centroid c_i and certain algorithm parameters, for example, a , A , and C as coefficient vectors.

3.4.2.2. Fitness Evaluation. In every square of the image we continue to find the fitness F_i in a portioned part and here the fitness is the most extreme precision of the fragmented part. The precision is discovered utilizing the parameters, for example, True Positive (TP), True Negative (TN), False Positive (FP) and False Negative (FN).

3.4.2.3. Separate the Solution Based on the Fitness. Now, we find the separate solution (threshold) based on the fitness value. Let the first best fitness solutions be α , the second best fitness solutions β and the third best fitness solutions δ .

3.4.2.4. Update the Position. We assume that the alpha (best candidate solution), beta and delta have the improved knowledge about the potential location of the prey in order to reproduce mathematically the hunting behavior of the grey wolves. As a result, we hoard the first three best solutions attained so far and require the other search agents (including the omegas) to revise their positions according to the position of the best search agent. For repetition, the new solution $c(t+1)$ is estimated by using the formulae mentioned below.

$$D^\alpha = |C_1 \cdot c_\alpha - c|, \quad D^\beta = |C_2 \cdot c_\beta - c|, \quad D^\delta = |C_3 \cdot c_\delta - c| \quad (20)$$

$$c_1 = c_\alpha - A_1 \cdot (D_\alpha), \quad c_2 = c_\beta - A_2 \cdot (D_\beta), \quad c_3 = c_\delta - A_3 \cdot (D_\delta) \quad (21)$$

To have hyper-spheres with different random radii, the arbitrary parameters A and C help the candidate solutions. Examination and usage are ensured by the adaptive estimations of A and a . The adaptive estimations of the parameters A and a license the GWO to travel them easily among the investigation and the usage. With diminishing A , half of the iterations are committed to the investigation ($|A| < 1$) and the other half are dedicated to the usage. Enclosing the conduct, the subsequent equations are utilized keeping in mind the end goal to give numerical model.

$$D = |C \cdot c_p(t) - c(t)| \quad (22)$$

The coefficient vectors are found by the Eq. (28)

$$A = 2a \cdot r_1 - a, \quad C = 2 \cdot r_2 \quad (23)$$

Where t indicates the current iteration, A and C are coefficient vectors, c_p is the position vector of the prey c and indicates the position vector of a grey wolf. The components of a are linearly decreased from 2 to 0 over the course of iterations and r_1, r_2 are random vectors in $[0, 1]$.

The GWO has only two main parameters (A and C) to be adjusted. However, we have kept the GWO algorithm as simple as possible with the fewest operators to be adjusted. The process will be continued until the maximum accuracy is obtained.

3.4.3. Optimal Centroid to the FCM

The last process is the segmentation process is the value that is attained from the optimal centroid computation process leads to a precise extorted tumor part of the image.

4. RESULTS AND DISCUSSION

The proposed brain tumor classification and segmentation are experimented in the working platform of MATLAB 2014 with the system configurations as i5 processor with 4GB RAM and the evaluation is done in respect of the classification as well as the segmentation. Subsequently in the segmentation, the performance evaluation is carried out in terms of the sensitivity, specificity, accuracy, Random Index, Global Contingency Error (GCE) and the Variation of Information (VI). The ANFIS technique is utilized to classify the tumor part of the image and the FCM with the GWO technique being employed to predict the centroid which produces better results. The proposed work is compared to the existing work in terms of the parameters like the sensitivity, specificity and accuracy.

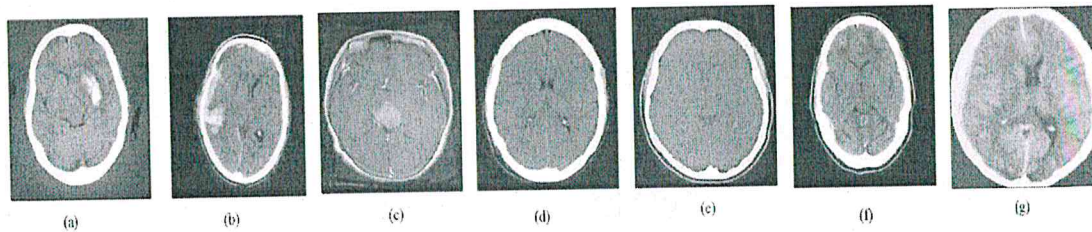


Fig. 5. Sample brain images.

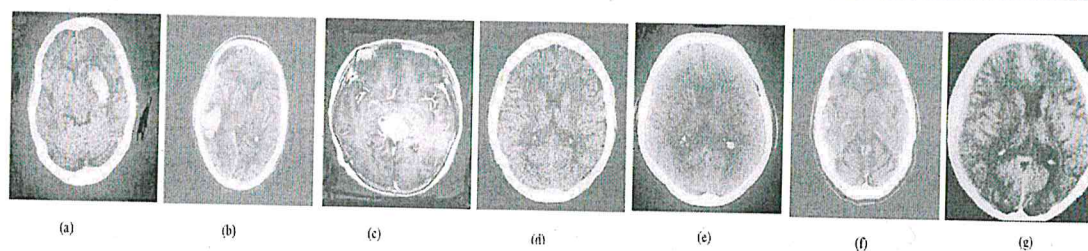


Fig. 6. Noise removal brain image.

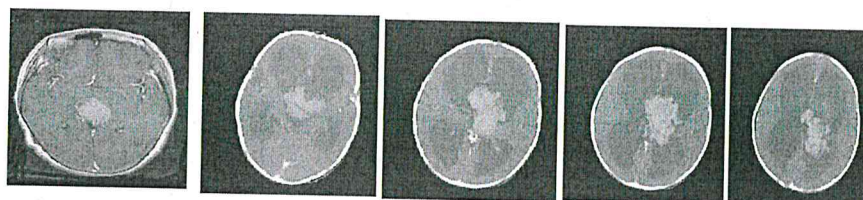


Fig. 7. Classification images.

4.1. CT Image Dataset Description

The CT image dataset employed in the innovative tumor detection approach is compiled from the public accessible sources and it encompasses the brain CT images including the tumor and non-tumor images. The CT image dataset that we have utilized in our proposed tumor detection technique is collected from M/s Aarthi scans (3D Multi slice CT scanner), Tirunelveli, India. This image dataset contains brain CT images which involve both tumor images (205 numbers) and non-tumor images (78 numbers). The data set of brain images, in essence, is divided into two distinct segments like the training and testing datasets. The training dataset, in turn, is effectively employed to fragment the brain tumor images where as the testing dataset elegantly executes the function of assessing the efficiency in the performance of the novel method technique. Figure 5 illustrates a sample of the CT brain images including tumor and non-tumor images. Further, Figure 6 depicts the picture of the noise elimination of the brain image effectively utilizing the filter. This image database is collected from UCI database and the resolution is 640×480 .

4.2. Experimental Results of Classification Process

This section well furnishes the test outcomes of the classification procedure on the brain CT images. In the CT images, the tumor and the non-tumor segments are classified with the help of the ANFIS classifier. The novel approach is well-geared to classify the tumor and the non-tumor segments in an effectual manner. The ensuing figure exhibits the CT test images with the authentication procedures guaranteeing superb precision.

Figure 7 stylishly exhibits that the classification procedure authentication images, which encompass both the brain normal and abnormal images, in which the precision of the novel method is far superior to those of the parallel modern approaches. Figure 8 elegantly exhibits the precision of various techniques assessed and contrasted with the ANFIS technique which also ranks the novel approach at the top of the list in terms of precision. The Back propagation neural network (BNN) precision when compared to the innovative approach the precision

divergence is 30.23% whereas in the case of racial bias function in comparison with the ANFIS technique, the divergence in precision is only 15.36%. In an identical manner, certain significant differences exist between the ANFIS and the network functions in the classification authentication procedures.

4.3. Segmentation Performance

In the segmentation procedure, the tumor part is fragmented by the novel approach viz. FCM with the centroid optimization employing the Grey Wolf Optimization (GWO). In Table I, the original CT images housing the tumor and the fragmented tumor part of the CT images are effectively exhibited. In the testing stage, the test dataset is furnished to the innovative method for the purpose of locating the tumors in brain images and the outcomes are achieved. The segmentation task includes the original image, the classified tumor image and fragmented image along with the performance measures like the Sensitivity, Specificity, Accuracy, Random Index, Global Contingency Error (GCE) and the Variation of Information (VI). These evaluations are expressed in terms of various parameters such as the True Positive (TP), True Negative (TN), False Positive (FP) and the

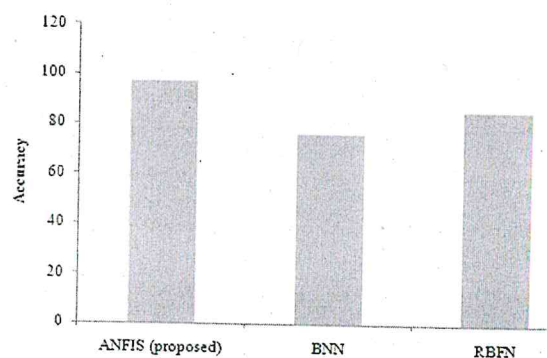


Fig. 8. Classification accuracy for different methods.

Table I. Segmentation results of proposed and existing methods with accuracy.









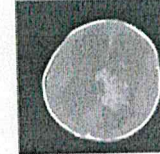

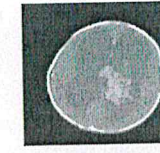

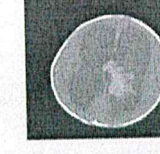
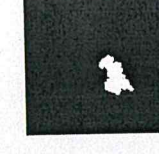

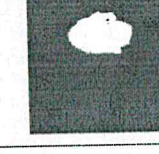


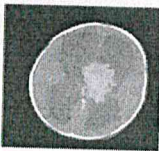

Sl. no	Original image	Segmented image	Accuracy		
			FCM-GWO (proposed)	FCM (existing)	Manual (%)
1			99.296%	58.711%	42.53
2			99.424%	55.466%	32.589
3			99.1294%	55.8048	60.23
4			99.24%	56.72	50.23
5			99.1065	56.865	77.82
6			98.23%	55.56%	78.23
7			92.23%	58.23%	81.23
8			89.23%	59.62%	45.27

Table I. Continued.

Sl. no	Original image	Segmented image	Accuracy		
			FCM-GWO (proposed)	FCM (existing)	Manual
9			89.97 %	57.28 %	55.21
10			98.52 %	61.29 %	60.23

False Negative (FN). Segmentation results are validated in MATLAB 2015a in FCM segmentation technique.

TP: tumor part correctly marked as tumor

TN: normal area correctly unmarked as tumor

FP: normal area wrongly marked as tumor

FN: tumor area wrongly unmarked as tumor.

Table I shows the accuracy comparison for proposed optimized FCM model; existing FCM and manual segmentation process are considered. Manual segmentation results are compared proposed work its minimum accuracy is obtained.

The evaluation of brain tumor detection in different images is carried out by applying the following equations.

Sensitivity: Sensitivity is a measure which determines the probability of the results that are true positive as 'that person has the tumor.'

Sensitivity

$$= \frac{\text{Number of True Positives}}{\text{Number of True Positives} + \text{Number of False Negatives}} \quad (24)$$

Specificity: Specificity is a measure which determines the probability of the results that are true negative as 'that person does not have the tumor.'

Specificity

$$= \frac{\text{Number of True Negatives}}{\text{Number of True Negatives} + \text{Number of False Positives}} \quad (25)$$

Accuracy: Accuracy is a measure which determines the probability that how many results are accurately classified.

$$\text{Accuracy} = \frac{TP + TN}{TP + TN + FP + FN} \quad (26)$$

Random Index (RI): Rand index calculates the fraction of pairs of pixels labeling that they become steady between the computed segmentation and the ground truth. The Rand index or Rand measure is a calculation of the similarity between the two clusters.

$$RI = \frac{a+b}{a+b+c+d} \quad (27)$$

Where, $a+b$ is the number of agreements between the partitions X and Y and $c+d$ is the number of disagreements between the partitions X and Y .

Global Consistency Error (GCE): GCE measures the extent to which segmentation can be viewed as a refinement of the other. Segmentation is simply a division of the pixels of an image into sets.

$$GCE = \frac{1}{n} \min \left\{ \sum_i E(S_1, S_2, p_i), \sum_i E(S_2, S_1, p_i) \right\} \quad (28)$$

Where segmentation error measure takes two segmentations S_1 and S_2 as input, these values contain pixel.

Table II. Statistical performance measures of FCM and FCM-GWO.

Image no	Sensitivity		Specificity		RI		GCE		VI	
	FCM-GWO	FCM	FCM-GWO	FCM	FCM-GWO	FCM	FCM-GWO	FCM	FCM-GWO	FCM
1	0.9365	0.045	0.993	0.9	0.985	0.363	0.013	0.013	0.170	3.677
2	0.931	0.049	0.9955	1	0.988	0.333	0.010	0.021	0.193	3.992
3	0.883	0.071	0.9953	1	0.98	0.349	0.018	0.025	0.339	4.058
4	0.9722	0.091	0.9932	1	0.983	0.369	0.01	0.023	0.3245	3.975
5	0.946	0.061	0.992	1	0.981	0.350	0.017	0.026	0.2241	3.875
6	0.9721	0.051	0.94	1	0.94	0.351	0.01	0.026	0.22	4.81
7	0.941	0.091	0.92	1	0.98	0.369	0.01	0.024	0.28	4.92
8	0.952	0.049	1	1	0.98	0.371	0.09	0.026	0.24	4.21
9	0.97	0.015	2.3	0.9	0.99	0.363	0.07	0.028	0.22	4.56
10	0.90	0.014	2.9	1	0.92	0.39	0.01	0.085	0.35	3.56

Variation of Information (VI): The VOI metric defines the distance between the two segmentations as average conditional entropy of one segmentation to the other.

$$VI(X; Y) = H(X) + H(Y) - 2I(X, Y) \quad (29)$$

Where, $H(X)$ is entropy of X and $I(X, Y)$ is mutual information between X and Y .

Tables I and II show the segmented brain tumor parts of the images with various statistical performance measures of the segmented images. The proposed methodology is compared to the normal FCM process to get the better performance measures. The maximum accuracy of the segmented image is 99.42% in image 2 compared to that of the existing process. Regarding the specificity measure, when the images numbered 2, 3 and 4 are taken as samples, the value thus obtained by using the GWO is 99.23% whereas the value attained by using the other two techniques is 98%. Other performance evaluation measures of the tumor segmentation process such as the sensitivity and specificity process is 99.3 and 93.6 in the FCM with the centroid optimization process. In respect of all the statistical parameters the better result is produced in the FCM-GWO compared to the FCM. Further, the GCE factor shows the minimum error in the suggested method. The random index of image 5 in the proposed method is 98% and when compared to the FCM the difference is 64.23% and a similar difference is produced in all the parameters. Hence, overall, the suggested method has a specified accuracy of 99.05% compared with the other techniques.

4.3.1. Comparative Analysis

The Figure 9 shows that the convergence graph is plotted between the iteration and fitness estimations of the various strategies, for PSO, GWO, and ACO. This graph basically resolves that the GWO procedure is given the greatest fitness using least possible iteration. Through the graph, the GWO Strategy takes the minimum iteration for providing the ideal result. Subsequently, it is maximized to 98.65% and it's attained in 87 iterations. Then the iteration is varied the performance also changing in all techniques. When the maximum fitness of the GWO technique contrasted with the PSO the estimation is 92.56. When contrast with the ACO the estimation are 87.28. Through the graph the grey

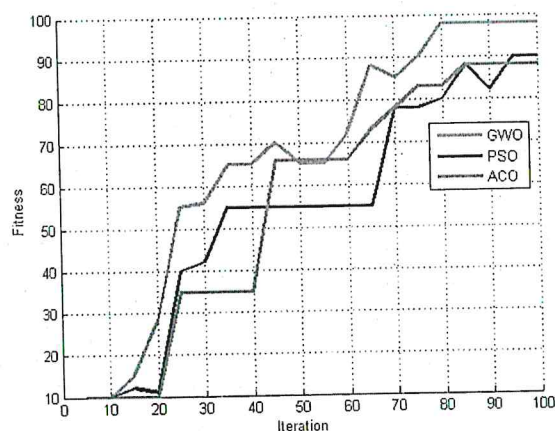


Fig. 9. Comparative analysis.

wolf Optimization strategy just specifies the ideal fitness value with the efficient results.

5. CONCLUSION

The tumor image segmentation and classification constitute the two vital daunting challenges in the medical image segmentation. In the document, an earnest effort is made to flag off an efficient tumor detection technique for the brain CT Images employing ANFIS with an eye on classifying the tumor and non-tumor images. It is followed by the task of the optimization of the FCM in relation to the segmentation procedure. In the document, the Grey Wolf Optimization (GWO) is effectively employed to fragment the tumor part in the segmentation section to fine-tune the segmentation function. The outcomes for the tumor recognition are authenticated by means of the estimation tools such as the sensitivity, specificity and the accuracy. The convincing outcomes achieved illustrate that the novel ANFIS classifier achieves a precision of a whopping 97.23% whereas the FCM with the centroid optimization approach tops the list with an amazing precision of 99.24%. The current investigation is used for the purpose of fine-tuning the efficiency of the parallel classifiers rather than that of ANFIS approach in perking up the precision. Still, the superb precision level of the novel approach underscores the fact that the proposed algorithm graph is significantly effective in identifying the tumors in the brain CT images.

References and Notes

1. I. Chiuchisan, A new FPGA-based real-time configurable system for medical image processing, *Proceedings of Conference on E-Health and Bioengineering* (2013), pp. 21–23.
2. P. Kaur, I. M. S. Lamba, and A. Gosain, A robust method for image segmentation of noisy digital images, *The Proceedings of IEEE International Conference on Fuzzy Systems* (2011), pp. 1656–1663.
3. Eman Abdel-Maksoud, Mohammed Elmogy, and Rashid Al-Awadi, Brain tumor segmentation based on a hybrid clustering technique, *Journal of Egyptian Informatics* 1 (2015).
4. M. Gandhi and R. Dhanasekaran, Diagnosis of diabetic retinopathy using morphological process and SVM classifier, *Conference on Communication and Signal Processing* (2013), pp. 873–877.
5. MarjanLaal, Innovation Process in Medical Imaging, *Journal of Procedia Social and Behavioral Sciences* 81, 60 (2013).
6. R. Vardasca and R. Simoes, Current issues in medical thermography, *Journal of Medical Image Processing and Computational Vision* 223 (2013).
7. X. Yang, C. Shao, R. Wang, C.-Y. Chu, P. Hu, V. Master, AdeboyeOsunkoya, H. Kim, HaiyenZhou, and L. Chung, Optical imaging of kidney cancer with novel near-infrared heptamethinecarbocyanine fluorescent dyes, *Journal of Urology* 1 (2012).
8. S. Talu, Multifractal geometry in analysis and processing of digital retinal photographs for early diagnosis of human diabetic macular edema, *Journal of Eye Research* 38, 781 (2013).
9. AlexandreBernardes, J. Rogeri, R. Oliveira, NorianMarranghello, A. Pereira, A. Araujo, and J. M. Tavares, Identification of foliar diseases in cotton crop, *Journal of Medical Image Processing and Computational Vision* 67 (2013).
10. P. Fossati, Neural correlates of emotion processing: From emotional to social brain, *Journal of European Neuropsychopharmacology* 22, 487 (2012).
11. M. N. Servaas, J. van der Velde, S. G. Costafreda, P. Horton, J. Ormel, H. Riese, and A. Aleman, Neuroticism and the Brain: A quantitative meta-analysis of neuroimaging studies investigating emotion processing, *Journal of Neuroscience and Biobehavioral Reviews* 1 (2013).
12. L. A. Bezerra, M. M. Oliveira, T. L. Rolim, A. Conci, F. G. S. Santos, P. R. M. Lyra, and R. C. F. Lima, Estimation of breast tumor thermal properties using infrared images, *Journal of Signal Processing* 93, 2851 (2013).
13. A. Mittal and S. K. Dubey, Analysis of MRI images of rheumatoid arthritis through morphological image processing techniques, *Journal of Computer Science* 10, 118 (2013).
14. J. Schulz-Menger, D. Bluemke, J. Bremerich, S. Flamm, M. Fogel, M. Friedrich, R. Kim, Florian von Knobelsdorff-Brenkenhoff, C. Kramer, D. Pennell, S. Plein, and EikeNagel, Standardized image interpretation and

- post processing in cardiovascular magnetic resonance: Society for cardiovascular magnetic resonance (SCMR) board of trustees task force on standardized post processing. *Journal of Cardiovascular Magnetic Resonance* 1 (2013).
15. A. Valli and G. W. Jiji, Parkinsons disease diagnosis using image processing techniques a survey. *Journal on Computational Sciences and Applications* 4, 57 (2014).
 16. F. Rousseau, Estanislao Oubel, Julien Pontabry, M. Schweitzer, C. Studholme, Meriam Koob, and J.-L. Dietemann, BTK: An open-source toolkit for fetal brain MR image processing. *Journal of Computer Methods and Programs in Biomedicine* 109, 65 (2013).
 17. T. Schramm, A. Hester, I. Klinkert, J.-P. Both, R. M. A. Heeren, A. Brunelle, O. Laprevote, N. Desbenoit, M.-F. Robbe, M. Stoeckli, B. Spengler, and A. Rompp, imzML—A common data format for the flexible exchange and processing of mass spectrometry imaging data. *Journal of Proteomics* 75, 5106 (2012).
 18. C. Tsotsios and M. Petrou, On the choice of the parameters for anisotropic diffusion in image processing. *Journal of Pattern Recognition* 46, 1369 (2013).
 19. L. Walker, L. C. Chang, A. Nayak, M. O. Irfanoglu, K. N. Botteron, J. McCracken, R. C. McKinstry, M. J. Rivkin, D. J. Wang, J. Rumsey, and C. Pierpaoli, The diffusion tensor imaging (DTI) component of the NIH MRI study of normal brain development (PedsDTI). *Journal of NeuroImage* 1 (2015).
 20. Tayade, Wankhede, Bhamare, and Sabale, Role of image processing technology in healthcare sector: Review. *Journal of Healthcare and Biomedical Research* 2, 8 (2014).
 21. C. Bhuvaneswari, P. Aruna, and D. Loganathan, Classification of lung diseases by image processing techniques using computed tomography images. *Journal of Advanced Computer Research* 4, 87 (2014).
 22. A. Mishra, A. Rai, and A. Yadav, Medical image processing: A challenging analysis. *Journal of Bio-Science and Bio-Technology* 6, 187 (2014).
 23. S. N. Chavan and A. M. Sutkar, Malaria disease identification and analysis using image processing. *Journal of Latest Trends in Engineering and Technology* 3, 218 (2014).
 24. C. L. Hung and Y. H. Wu, Parallel genetic-based algorithm on multiple embedded graphic processing units for brain magnetic resonance imaging segmentation. *Journal of Computers and Electrical Engineering* 1 (2016).
 25. I. Despotović, B. Goossens, and W. Philips, MRI segmentation of the human brain: Challenges, methods, and applications. *Journal of Computational and Mathematical Methods in Medicine* 1 (2016).

Received: 31 May 2016. Revised/Accepted: 3 December 2016.